Journal of Materials Chemistry B

Accepted Manuscript

ROYAL SOCIETY OF CHEMISTRY

www.rsc.org/materialsB

Journal of Materials Chemistry B

ARTICLE

Novel protein-loaded chondroitin sulfate-N-[(2-hydroxy-3-trimethylammoniumpropyl)chitosan nanoparticles with reverse zeta potential: Preparation, characterization, and ex vivo assessment

Received 00th January 20xx,
Accepted 00th January 20xx

DOI: 10.1039/x0xx00000x

www.rsc.org/

Tsung-Neng Tsai,[a] Hui-Ju Yen,[b,c] Cheng-cheung Chen,[b] Ying-chuan Chen,[b,d] Yen-an Young,[e] Kuang-ming Cheng,[b] Jenn-jong Young*[b] and Po-da Hong[c]

A facile polyelectrolyte complexation method for the preparation of both positively and negatively surface charged nanoparticles composed of chondroitin sulfate (ChS) and N-[(2-hydroxy-3-trimethylammonium)propyl]chitosan (HTCC) is reported. Production of ChS-HTCC nanoparticles with reverse zeta potential was easily controlled by varying the ChS/HTCC mass ratio. The encapsulation efficiency increased with an increase in initial FITC-BSA concentration in positively charged NPs and reached 75%. However, a maximum of 20% encapsulation efficiency was achieved in the case of negatively charged NPs. In vitro release studies of positively charged ChS-HTCC NPs showed a small burst effect followed by a continued and controlled release. Both charges of ChS-HTCC NPs showed no cytotoxicity in HUVEC cells. The confocal images showed that ChS-HTCC NPs of both charges can be incorporated and retained by the A549 cells. Flow cytometric analysis data demonstrated that ChS-HTCC NPs of both charges were detected in more than 80% of the A549 cells.

1. Introduction

Chitin is a major component of the shells of crustaceans such as shrimp, crab, and crawfish and is the second most abundant naturally occurring polysaccharide after cellulose. Chitosan (CS), the deacetylated product of chitin, is composed of 2-amino-2-deoxy-β-D-glucan combined with glycosidic linkages. As a natural renewable resource, chitosan has several unique biological properties such as nontoxicity, biodegradability, biocompatibility, antimicrobial activity, and muco-adhesiveness, which attracts scientific and industrial interest for its potential applications in pharmaceutics, food science, cosmetics, textiles, and biotechnology. Compared to many other natural polymers, CS has primary amino groups that can confer positive charges and special chemical properties that make it very useful in pharmaceutical applications.[1] However, chitosan has not been fully utilized because of its low solubility in neutral and alkaline aqueous solution.

Quaternary chitosan, a chitosan derivative with permanent cationic charges on the polysaccharide backbone, becomes water-soluble over a wide range of pH values and exhibits antimicrobial activity.[2] N-[(2-hydroxy-3-trimethylammonium propyl)chitosan chloride (HTCC) is one of the water-soluble quaternary ammonium salts of chitosan, is easily prepared via coupling chitosan with glycidyl trimethylammonium chloride (GTMAC),[3] has good moisture-retention capacity, and has better antimicrobial[4,5] and antioxidant activity[6] than unmodified chitosan.

Osteoarthritis is a debilitating disease caused by a gradual loss of articular cartilage in synovial joints that causes painful impairment. The pharmacological therapy is directed towards the prevention of pain and the improvement of function. Standard analgesic/anti-inflammatory drugs exert various gastrointestinal and cardiovascular side effects and do not repair degenerated connective tissue.[7] Chondroitin sulfate (ChS) proteoglycans are principal pericellular and extracellular components that form regulatory milieu involving numerous biological and pathophysiological phenomena. Oral supplementation of ChS helps to preserve and repair the damage to the articular surface caused by osteoarthritis by reducing the concentration of pro-inflammatory cytokines and transcription factors.[8] ChS is commercially available as a dietary supplement for the prevention of cartilage loss.

[a] Division of Cardiology, Department of Internal Medicine, Tri-Service General Hospital, National Defense Medical Center, No. 325, Sec. 2, Cheng-gong Rd., Neihu Dist., Taipei City 11490, Taiwan, ROC.
[b] Institute of Preventive Medicine, National Defense Medical Center, PO Box 90048-700, Sanhsia Dist., New Taipei City 23742, Taiwan, ROC. E-mail: jjyoung@ms49.hinet.net
[c] Biomedical Engineering Program, Graduate Institute of Applied Science and Technology, National Taiwan University of Science and Technology, Taipei City 10607, Taiwan, ROC.
[d] Department of Physiology & Biophysics, National Defense Medical Center, No. 161, Section 6 Min-Chuan East Road, Neihu Dist., Taipei City 11490, Taiwan, ROC.
[e] Department of Applied Chemistry, National Chiao-Tung University, 1001 University Road, Hsinchu 300, Taiwan, ROC

†Electronic Supplementary Information (ESI) available: The effect of mass ratio between anionic polyelectrolyte and cationic polyelectrolyte on the particle size and zeta potential of ChS-HTCC NPs and ChS-CS NPs (Figure S1). See DOI: 10.1039/x0xx00000x

Negatively charged ChS is capable of electrostatic interaction with positively charged growth factors to stabilize and prevent degradation of the growth factors in medium.[9,10] Therefore, ChS may be a promising carrier for delivery of cationic growth factors to induce cell adhesion, differentiation, and migration and to direct differentiation of stem cells.[11,12]

It has been shown that nano-size particles exhibit dramatically prolonged residence time in the gastrointestinal tract by decreasing the influence of intestinal clearance mechanisms. However, the surface characteristics of these nanoparticles (NPs), including their hydrophilicity, chemistry, and surface charge, also play important roles in cell adhesion. CS NPs have garnered much attention in recent years because of their ability to adhere to the mucosal surface[13] and transiently open tight junctions between epithelial cells.[14] CS NPs were first prepared by Calvo et al.[15,16] and were based on the ionic gelation of CS with sodium tripolyphosphate (TPP) anions. The hydrophilic CS NPs generally circulate longer in the blood. Such systems could be used to control the rate of drug administration, prolonging the duration of the therapeutic effect and also helping to deliver the drug to specific sites. Chitosan has also been reported to form nano-complexes with different anionic natural polyelectrolytes, such as alginate,[17] heparin,[18] hyaluronic acid,[19] and ChS,[20] by PEC methods. Among these nano-carrier systems, ChS-CS nanoparticles contain hydrophilic three-dimensional (3D) polymeric networks that can absorb much more water than their own weight and function as an ideal matrix for biocompatible applications and for environmentally sensitive bioactive materials such as growth factors.[21,22] However, ChS-CS nanoparticles must be formed under acidic conditions (pH below 6.5), limiting their applications in the delivery of acid-sensitive proteins and drugs.

In the present paper, we successfully developed a new type of hydrophilic NP with positive or negative surface charges obtained from ChS and HTCC in a neutral aqueous solution. We investigated the formation zone of positively and negatively charged NPs under different addition processes. We also measured their particle size, zeta potential, formation yield, and water content at different ChS/HTCC weight ratios and concentrations. Subsequently, the efficacy of reverse-charged ChS-HTCC NPs for the entrapment and controlled release of proteins was evaluated in vitro. Also, the ex vivo cytocompatibility and cellular uptake ability of both charged ChS-HTCC NPs were investigated.

2. Experimental

2.1. Materials

Chitosan (viscosity: 3.6 mPa · s [5 g/L], degree of deacetylation [DD]: 93.8%) was purchased from Wako Pure Chemical Industries, Ltd. (Osaka, Japan). Chondroitin 4-sulfate sodium salt (ChS) from bovine trachea and glycidyl trimethylammonium chloride (GTMAC) were provided by Fluka (Buchs, Switzerland). Fluorescein isothiocyanate (FITC) and fluorescein isothiocyanate conjugate bovine serum albumin (FITC-BSA) were obtained from Sigma (St. Louis, MO, USA). Antibiotics solution (100 IU/mL penicillin and 100 µg/mL streptomycin), fetal bovine serum (FBS), and phosphate-buffer saline (PBS), pH 7.4, were supplied by Gibco BRL (Corning, NY, USA). Glacial acetic acid was purchased from Merck (Darmstadt, Germany). Ultra-pure water was obtained with milli-Q equipment (Millipore, Billerica, MA, USA).

2.2. Synthesis of HTCC

The HTCC was synthesized according to a previous report[3] with minor modifications. Briefly, chitosan was suspended in milli-Q water at 80°C. GTMAC was dissolved in aqueous solution and added dropwise to a chitosan suspension with continuous stirring. The molar ratio of GTMAC to amino groups of chitosan was 4. After the reaction at 80°C for 20 h, the turbid and yellowish reaction solution was cooled to room temperature and poured into cold acetone. After washing with acetone and methanol, the precipitated product was re-dissolved in water and centrifuged (10,000×g, 20 min) to remove the un-dissolved portion. The clear supernatant was then poured into absolute ethanol with continuous stirring, and the white precipitated product was collected by centrifugation (10,000×g, 10 mins) again. To obtain more purified HTCC, the product was dialyzed (Slide-A-Lyzer® Dialysis Cassette G2, 2000 MWCO, 70 ml capacity) against water for 3 days and lyophilized.

The degree of quaternization (DQ) was determined by titrating the Cl^- ions with aqueous $AgNO_3$ and monitoring the solution conductivities.[23]

2.3. Synthesis of FITC-conjugated HTCC

FITC-conjugated HTCC (f-HTCC) was synthesized according to a method described by Huang et al.[24] with minor modifications. In brief, HTCC was dissolved in milli-Q water. FITC, previously dissolved in DMSO, was slowly added to the HTCC aqueous solution under continuous stirring. The reaction was carried out overnight at room temperature in the dark. The resulting solution was poured into an excess of acetone and then centrifuged for 10 min at 3,000 rpm. The pellet was washed several times with fresh acetone until no FITC fluorescence color was observed in the washing solution. The pellet was then dissolved in water and dialyzed against water using a Dialysis Cassette (Slide-A-Lyzer®, G2, 2000 MWCO, 70 ml capacity) for 3 days while protected from light. The f-HTCC was then lyophilized. To determine the labeling efficiency, a specified amount of the f-HTCC was dissolved in milli-Q water and the fluorescence intensity was measured using a spectrofluorometer (Fluoroskan Ascent, Thermo, Finland) at λ_{exc} 485 nm and λ_{emi} 520 nm.

2.4. Investigation of the aggregation zones of ChS-HTCC NPs

Positively or negatively charged ChS-HTCC NPs were prepared based on the PEC method of anionic polyelectrolyte ChS with cationic polyelectrolyte HTCC. Preliminary experiments were done in order to determine the aggregation zones of particle formation at different ChS/HTCC weight ratios (4/1, 2/1, 1.4/1, 1.2/1, 1.1/1, 1/1, 1/1.1, 1/1.2, 1/1.4, 1/2, and 1/4) and at the different final concentrations of HTCC (2, 1, and 0.5 mg/mL). Meanwhile, two different addition processes were investigated; Method A, the ChS solutions was added dropwise to the HTCC solutions, and method B, the HTCC solution was added dropwise to the ChS solutions. The particle size and zeta potential were measured at the different

weight ratios of ChS/HTCC and the final concentration of HTCC in order to determine the formation zone of the NPs suspension.

2.5. Preparation of ChS-HTCC or ChS-f-HTCC NPs and FITC-BSA encapsulation

Positively or negatively charged ChS-HTCC or ChS-f-HTCC NPs were formed spontaneously upon incorporation of ChS aqueous solution into HTCC or f-HTCC aqueous solution (or inverse) under magnetic stirring at room temperature. The agitation was maintained for 10 min in order to allow for stabilization of the system.

The FITC-BSA-loaded positively or negatively charged ChS-HTCC NPs were generated after mixing the FITC-BSA with ChS prior to NP formation.

2.6. Physicochemical characterization of ChS-HTCC NPs

The particle size was characterized by photon correlation spectroscopy (Zetasizer Nano-ZS; Malvern Instruments, UK). All measurements were performed at a wavelength of 633 nm at room temperature with a detection angle of 173°. Raw data were subsequently correlated to the mean hydrodynamic size by cumulant analysis (Z-average mean). The Zeta potentials of all NPs were analyzed using laser doppler anemometry (Zetasizer Nano-ZS; Malvern Instruments, UK). All samples were run in triplicate, and the mean averages and standard deviations were calculated.

NPs were separated from suspension by centrifugation (Model 3740; Kubota Corporation, Tokyo, Japan) at 20,000×g and 4°C for 30 min, and they were then dried using a freeze dryer. Their Fourier transform-infrared (FT-IR) spectra were taken with KBr pellets on a PerkinElmer Spectrum One FTIR (PerkinElmer, Waltham, MA, USA). NP morphology was examined on a Jeol JEM-1200EXII transmission electron microscopy (TEM; Jeol, Tokyo, Japan). A typical method for preparation of TEM samples was as follows: one drop of ChS-HTCC NPs suspension was deposited on a 200-mesh Formvar/carbon-coated copper grid, and excess solution was removed by wicking with filter paper to avoid particle aggregation. Samples were stained with 2% phosphotungstic acid and dried at room temperature.

2.7. Measurements of water content and formation yield

The water content and formation yield were measured by gravimetry. The NP suspensions were centrifuged at 20,000×g at 4°C for 30 min in pre-weighed centrifuge tubes, and wet weights (Ws) were determined after decanting the supernatant. The sediments were cooled to -70°C and lyophilized for 24 h, and the dry weights were measured again (Wd).

The water content and formation yield were calculated using equations (1) and (2), respectively, as indicated below:

$$\text{Water content (\%)} = [(W_s - W_d)/W_d] \times 100 \quad (1)$$

$$\text{Yield (\%)} = W_d/\text{Total weight (ChS + HTCC [+ FITC-BSA])} \times 100 \quad (2)$$

Where W_s is the weight of wet NPs and W_d is the weight of dry NPs.

2.8. Evaluation of loading capacity and encapsulation efficiency

The FITC-BSA-loaded NPs were separated from the aqueous suspension medium by centrifugation at 20,000×g and 4°C for 30 min. The amount of free FITC-BSA in the clear supernatant was analyzed using a spectrofluorometer (Fluoroskan Ascent, Thermo, Finland) at λ_{exc} 485 nm and λ_{emi} 520 nm. FITC-BSA at various known concentrations (2, 1, 0.5, 0.25, 0.125, 0.0625, and 0 mg/mL) served as the standard. Linear regression was performed with commercial statistical software on a personal computer.

The loading capacity (LC) and encapsulation efficiency (EE) of FITC-BSA were calculated from equations (3) and (4), as indicated below:

$$LC = (W_t - W_f)/W_d \times 100 \quad (3)$$

$$EE = (W_t - W_f)/W_t \times 100 \quad (4)$$

Where W_t is the total amount of FITC-BSA applied, W_f is the free amount FITC-BSA in the clear supernatant, and W_d is the weight of the dry NPs.

2.9. Evaluation of FITC-BSA release in vitro

The in vitro release of FITC-BSA from NPs was investigated according to the procedure reported by Calvo et al.,[15,16] with small modifications. Briefly, FITC-BSA-loaded ChS-HTCC NPs were placed into test tubes and incubated at 37°C in 8 mL of water or HEPES (pH 7.4). At appropriate intervals, the sample was vortexed and 0.5 mL of the suspension sample was taken and centrifuged at 20,000×g at 4°C for 30 min. The amount of FITC-BSA released from the NPs was analyzed for fluorescence using a spectrofluorometer at λ_{exc} 485 nm and λ_{emi} 520 nm.

To analyze the release kinetics and mechanisms, data were fitted to the four following mathematical models.[25,26]

1. Zero order

$$M_t/M_\infty = k_o \cdot t$$

2. First order

$$M_t/M_\infty = 1\text{-}\exp(-k_1 \cdot t)$$

3. Higuchi model[27-29]

$$M_t/M_\infty = k_h \cdot t^{1/2}$$

4. Power law model[29]

$$M_t/M_\infty = k \cdot t^n$$

Where M_t/M_∞ is the fraction of drug released at time t, and k_o, k_1, k_h, and k represent the zero-order release constant, first-order release constant, Higuchi constant, and Korsemeter-Peppas constant,[30] respectively. The constants are related to the structural and geometric characteristic of the device, and n is the swelling exponent, indicative of the drug release mechanism. For spheres, a value of n between 0.43 and 0.85 is an indication of both diffusion-controlled drug release and swelling-controlled drug release (anomalous transport). Values above 0.85 indicate Case-II transport, which relates to polymer relaxation during hydrogel swelling. Values below 0.43 indicate that drug release from the polymer was due to Fickian diffusion.[31,32] The values of k_o, k_1, k_h, k, and n were determined by fitting the release data to the respective equations.

2.10. Cell culture

Human umbilical vein endothelial cells (HUVECs) were purchased from Lonza, (Walkersville, MD, USA) and cells from the human lung adenocarcinoma epithelial cell line (A549) were obtained from American Type Culture Collection (Rockville, MD, USA). HUVECs were cultured in endothelial growth medium (EGM-2, Lonza,

Walkersville, MD, USA) and A549 cells were cultured in Dulbecco's Modified Eagle's Medium (Invitrogen, Carlsbad, CA) supplemented with 10% fetal bovine serum, 100 IU/mL penicillin, and 100 µg/mL streptomycin. Both cells were maintained at 37°C in a 5% CO_2 environment for the experiment. For the detection of cell viability, HUVECs were seeded on 96-well culture plates (Greiner Labortechnik, Frickenhausen, Germany). To assay the cell uptake by confocal microscopy scan and flow cytometry analysis, A549 cells were plated on 8-well Lab-Tek II Chamber Slides (Nalge Nunc, Elkhart, IN, USA) and 6-well culture plates (Greiner Labortechnik, Frickenhausen, Germany), respectively.

2.11. Ex vivo cell viability assay

Cell viability was evaluated by MTS (3-(4,5-dimethylthiazol-2-yl)-5-(3-carboxy- methoxyphenyl)-2-(4-sulfophenyl)-2H-tetrazolium) assay and performed according to the manufacturer's protocol. In brief, 5×10^3 HUVECs were seeded in a series of wells in a 96-well plate. Then, cells were incubated with various concentrations of positively or negatively charged ChS-HTCC NPs (0, 3.5, 7, 14, and 28 µg/ml), followed by the addition of 20 µl MTS tetrazolium compound reaction solution. Then, the samples were cultured in a CO_2 incubator at 37°C for 60 min. The absorbance was measured at 490 nm using an enzyme-linked immunosorbent assay reader (Thermo Scientific).

2.12. Ex vivo uptake detected by confocal microscopy

To detect the uptake of both charged ChS-HTCC NPs by cells, A549 cells were incubated for 24 h with 7 µg/ml of ChS-f-HTCC NPs. Then, the cells were washed twice with phosphate buffered saline and fixed in a 3.7% paraformaldehyde-PBS solution for 10 min at room temperature. After two additional washes with PBS, cells were permeabilized with 0.1% Triton X-100 in PBS for 5 min and washed with PBS again. Texas Red-X phalloidin (Invitrogen, Carlsbad, CA) was used to localize filamentous actin (F-actin) which represents the cytoplasm of the cells. Nucleoli were stained with TOTO-3 (Molecular Probes, Eugene, OR). Fluorescent dyes were diluted in blocking solution (1% bovine serum albumin and 0.025% saponin in PBS) and added to coverslips for 90 min at room temperature. After three washes with PBS, coverslips were mounted with Prolong Gold antifade reagent (Life Technologies). Images were taken with a confocal laser scanning microscope (ZEISS LSM510).

2.13. Flow cytometric analysis

To quantify the efficacy of endocytosis of both charged ChS-f-HTCC NPs, analyses were performed using flow cytometry. The treatment steps for A549 cells were the same as described in the confocal microscopy section. Briefly, a million treated cells from each sample were trypsinized, washed, and analyzed using flow cytometry (Millipore, Billerica, MA, USA). Cells treated with ChS-HTCC NPs were used as a negative control.

3. Results and discussion

3.1. The formation of positively charged NPs, negatively charged NPs, and aggregates

The particle size and zeta potentials corresponding to the positively charged NPs, the negatively charged NPs, and the aggregates are illustrated in Figure 1 as a function of the ChS/HTCC mass ratio. The final concentrations of HTCC were in the range of 0.5–2 mg/ml. Aggregation only occurred in the range of the ChS/HTCC mass ratio approximately equal to one and at the final concentration of HTCC larger than 1 mg/ml. No aggregation phenomenon was observed at a final concentration of HTCC less than or equal to 1 mg/ml. Additionally, a smaller particle size NP was obtained at the lower final concentration of HTCC. The addition sequence of polyelectrolyte also had little influence on particle size. At the same HTCC final concentration, the addition method A resulted in smaller positively charged ChS-HTCC NPs, while addition method B resulted in smaller negatively charged ChS-HTCC NPs. Both addition methods showed the tendency for smaller particle sizes when closer to the aggregation point.

HTCC is a cationic polyelectrolyte, and our study was based on inducing its complexation by controlling its interaction with the counter ion ChS. The intermolecular linkages created between the negatively charged sulfate and carboxylate groups of ChS and the positively charged quaternary ammonium groups of HTCC are responsible for the success of the reverse-charged NPs formation. The ChS/HTCC mass ratios of positively charged ChS-HTCC NPs were less than or equal to 1/1.1, and that of the negatively charged ChS-HTCC NPs were greater than 1.1/1. Therefore, it can easily be predicted whether positively charged NPs, negatively charged NPs, or aggregates are formed by means of calculating the weight ratio of ChS/HTCC in the final suspension. The absolute value of the zeta potential was much smaller than 30 mV in the CS/HTCC mass ratio range between 1/1.1 and 1.1/1. This causes NPs with small electrostatic repulsive forces to stabilize in the aqueous medium, resulting in aggregate formation.

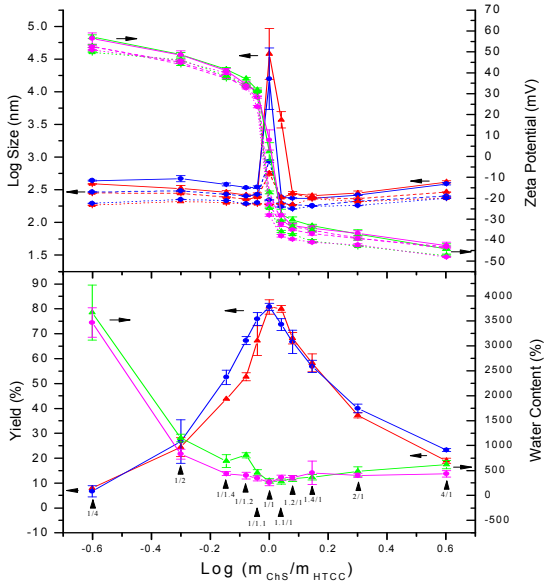

Figure 1. The effect of ChS/HTCC mass ratio on the particle size, zeta potentials, formation yield, and water content of ChS-HTCC NPs via two addition methods at different final concentrations of HTCC. (▲Method A; (●) Method B; Final concentration of HTCC: Solid line (2 mg/ml); Dash line (1 mg/ml); Dot line (0.5 mg/ml)

We dropwisely added the aqueous to a continuous stirring solution (~1000 rpm) by a micropipette, rather than a dropwise apparatus (such as: syringe pump). The addition rate is about 2 ml/minute. The pH of ChS aqueous is 6.8 and the pH of HTCC aqueous is 6.0. Although, the dropwise speed, the height between the needle and the collecting solution and the pore size of needle effect the particle size, however, the influence is very tiny, and it is difficult using a low resolution detection method (such as DLS and TEM) to distinguish the tiny difference in particle size.

3.2. The formation yield and water content of the positively charged and negatively charged NPs

Figure 1 also shows the influence of the ChS/HTCC mass ratio on the formation yield and water content of NPs. Both positively and negatively charged ChS-HTCC NPs showed a higher formation yield when the ChS/HTCC mass ratio was closer to the aggregation point, independent of addition methods. The water uptake ability of the NPs is a function of the degree of ionic cross-linking. Highly cross-linked NPs tend to show lower water content since the highly cross-linked 3D network cannot sustain much water within the network structure.33 All NPs show only a 5~10 fold increase in water uptake ability compared to their original weight except at the ChS/HTCC mass ratio below 1/2. This result indicated that a high cross-linking 3D network structure was formed between two polyelectrolytes. In the case of the ChS/HTCC mass ratio =1/4, because only low cross-linking density occurred, there was a 35 fold increase in water uptake ability compared to its original weight. The water contents of NPs were measured in milli-Q water rather than PBS, because the salts in PBS or other buffer systems will encapsulate in NPs and increased the dry weight of NPs, this phenomenon cause inconsistence water content value was measured.

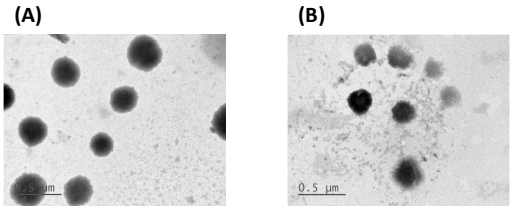

Figure 2. ChS-HTCC NPs with positive surface charge (A) and negative surface charge (B).

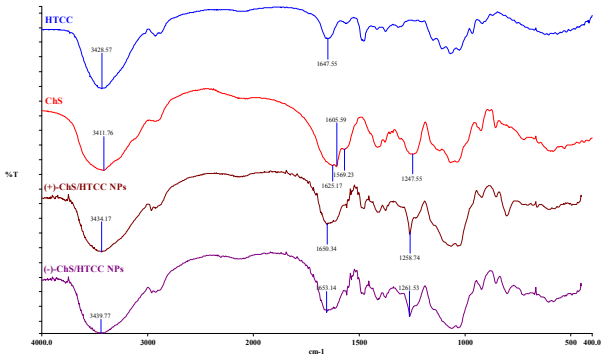

Figure 3. FTIR spectra of HTCC, ChS, positively charged ChS-HTCC NPs, and negatively charged ChS-HTCC NPs(C).

3.3. Characterization of the NPs

TEM images of the positively charged and negatively charged ChS-HTCC NPs are shown in Figure 2. The TEM images of both charged CS-HTCC NPs showed a dense, well-defined, spherical structure, which were consistent with the particle size measured by the dynamic light scattering method.

FT-IR spectra were analyzed to characterize the potential interactions in the NPs. Figure 3 shows the FT-IR spectra of pure HTCC, ChS, positively charged ChS-HTCC NPs, and negatively charged ChS-HTCC NPs. The characterization peaks in the pure ChS spectrum are 3412 cm^{-1} (OH and NH_2 stretching), 1626 cm^{-1} (amide I band), 1609 cm^{-1} (asymmetric CO_2^- stretching), 1571 cm^{-1} (NH deformation), 1257 cm^{-1} (asymmetric SO_2 stretching), and 1122 cm^{-1} (symmetric SO_2 stretching). Both positively charged ChS-HTCC NPs and negatively charged ChS-HTCC NPs had similar FTIR spectrums. In ChS-HTCC NPs, the 1609 cm^{-1} peak of the asymmetric CO_2^- stretching shifted to 1653 cm^{-1}, and the 1257 cm^{-1} peak of the asymmetric SO_2 stretching shifted to 1261 cm^{-1}. These differences indicated that an ionic bond between the ammonium group in HTCC and sulfate and carboxylate groups in ChS had been formed.

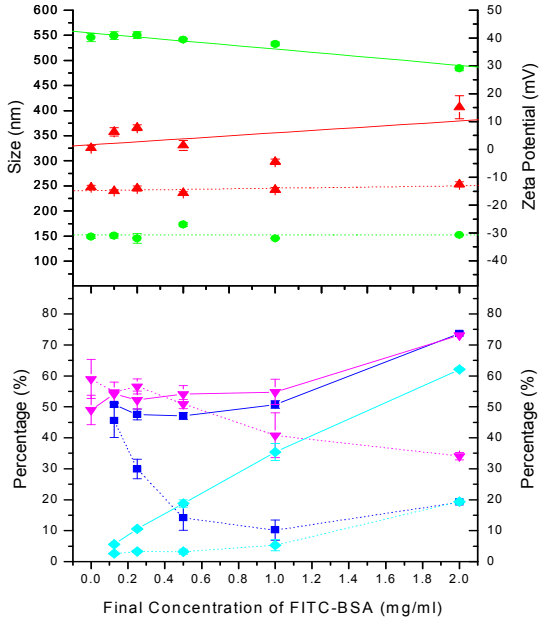

Figure 4. The effect of final concentration of FITC-BSA on the particle size, zeta potential, encapsulation efficiency, loading capacity, and formation yield of FITC-BSA encapsulated ChS-HTCC NPs with positive or negative surface charge. (▲) Size; (●) Zeta potential; (■) Encapsulation efficiency; (◆) Loading capacity; (▼) Yield; Solid line: ChS-HTCC NPs with positive surface charge; Dot line: ChS-HTCC NPs with negative surface charge.

3.4. Association of FITC-BSA to the positively charged and negatively charged ChS-HTCC NPs

The dependence of particles size, zeta potential, EE, LC, and formation yield of FITC-BSA-loaded NPs on the concentration of FITC-BSA is shown in Figure 4. In order to get a smaller particle size and higher formation yield of NPs, and to avoid aggregation in the process, the experiments were conducted by the incorporation

method using weight ratios of ChS/HTCC of 1/2 and 1/0.9 for the formation of FITC-BSA-loaded positively and negatively charged ChS-HTCC NPs, respectively. In the case of positively charged ChS-HTCC NPs, there was an increase in size, EE, LC, and yield with the increase in FITC-BSA concentration, and decreasing zeta potential with the increase in FITC-BSA concentration. Because FITC-BSA has a small isoelectric point (pI=4.92), the FITC-BSA processes negative charges in neutral conditions. These results indicated that a considerable amount of FITC-BSA was encapsulated in the positively charged ChS-HTCC NPs, and FITC-BSA played a part in the ionic cross-linking. However, in the case of negatively charged ChS-HTCC NPs, the FITC-BSA concentration had little influence on the size and zeta potential, and there was a decrease in EE and LC with increasing FITC-BSA concentration. This phenomenon was mainly due to the electrostatic repulsion force between the FITC-BSA and the surface charge of the NPs, and only a limited amount of FITC-BSA was encapsulated in the negatively charged ChS-HTCC NPs. Apparently, negatively charged ChS-HTCC NPs are not suitable carriers for protein with a negative charge. However, we predict that negatively charged ChS-HTCC NPs may be promising carriers for delivery of cationic growth factors.

3.5. In vitro release of FITC-BSA from the positively charged ChS-HTCC NPs

In many NP systems formed via the ionic gelation or PEC method of two counter ions, glycerol[34] or trehalose[15,16] are usually added to the suspension of NPs before centrifugation or freeze drying, to avoid aggregation formation, and re-dispersed in the medium with the NPs. The effect of medium and FITC-BSA concentration on the particles' size and zeta potentials of ChS-HTCC NPs re-dispersed from the centrifuged sediment was studied and the results are listed in Table 1. Positively charged FITC-BSA-loaded ChS-HTCC NPs can be easily re-dispersed in water and HEPES medium without adding any reagent to help the re-dispersion of centrifuged sediment, and a suspension was obtained with a large zeta potential and particle size less than 400 nm when the FITC-BSA concentration was less than or equal to 1 mg/ml. However, aggregates were formed after the PBS medium was added to the centrifuged sediment. This is mainly due to the phosphate ion participated in the ionic gelation process between two counter ions, destroying the stable positive surface charge of NPs.

Table 1. The effect of medium and FITC-BSA concentration on the particle size and zeta potentials of re-dispersion ChS-HTCC NPs from the centrifuged sediment.

FITC-BSA Conc. (mg/ml)	Original	Water	HEPES (pH 7.4)	PBS (pH 7.4)
	Size (nm) *Zeta (mV)*	Size (nm) *Zeta (mV)*	Size (nm) *Zeta (mV)*	Size (nm) *Zeta (mV)*
2	272.0±21.1 *28.5±0.7*	431.64.4 *50.6±0.9*	423.4±3.4 *34.2±0.6*	1508.3±126.3 *-3.6±0.6*
1	232.7±9.8 *36.8±1.0*	336.7±2.4 *53.5±0.8*	358.2±3.8 *36.3±0.3*	481.5±27.4 *37.3±0.8*
0.5	259.2±7.2 *39.6±1.2*	394.4±2.3 *58.3±0.1*	343.5±0.9 *35.0±0.1*	17170.0±20594.7 *-6.1±0.6*
0.25	277.2±5.8 *39.7±2.0*	393.2±5.5 *55.4±0.4*	393.3±2.7 *31.3±0.2*	4432.7±1274.0 *-0.1±0.6*

Figure 5 displays the release profiles of FITC-BSA from positively charged ChS-HTCC NPs in water and HEPES (pH 7.4). In both mediums, a small burst release of about 26% (in water) and 24% (in HEPES) of FITC-BSA was observed within 1 h, and a slow and sustained release of about 36% (in water) and 45% (in HEPES) was observed by day 7. This may be attributed to the strong ionic interaction between the counter ion of FITC-BSA and HTCC. The 3D network structure made the ChS-HTCC NPs more stable and promoted the continued and controlled release of protein via diffusion and/or swelling release.

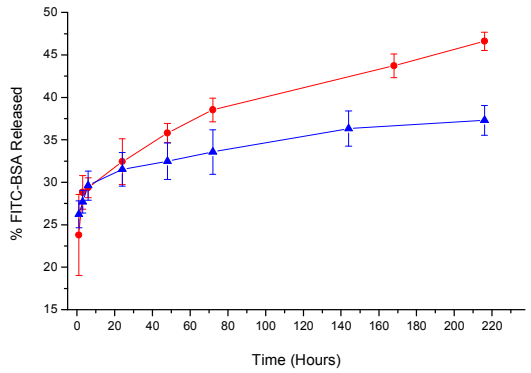

Figure 5. FITC-BSA release profile from FITC-BSA loaded ChS-HTCC NPs in water (▲, medium, and HEPES (pH 7.4) (●) at 37°C. Final concentration: ChS (1.2 mg/mL); HTCC (2 mg/mL); FITC-BSA (1 mg/mL); Total volume: 8 mL.

Table 2. Release parameters for FITC-BSA encapsulated ChS-HTCC NPs obtained after fitting in vitro drug release data to four different mathematical models for FITC-BSA release kinetics.

Medium	Mathematical models for FITC-BSA release kinetics			
	Zero-order	First-order	Higuchi model	Power law
ChS-HTCC in H_2O	k_0 = 0.0045 R^2 = 0.827	k_1 = 0.00068 R^2 = 0.845	k_h = 0.767 R^2 = 0.956	k = 26.01 n = 0.063 R^2 = 0.981
ChS-HTCC in HEPES (pH 7.4)	k_0 = 0.089 R^2 = 0.886	k_1 = 0.0014 R^2 = 0.916	k_h = 1.499 R^2 = 0.974	k = 23.96 n = 0.114 R^2 = 0.966

Because the Power law model explains only 60% of the releasing data, in order to determine the mechanism of drug release from our formulation we analyzed four different kinetic models.[25,26] Table 2 represents the calculated values of release constants and release exponents (n) determined by fitting the release data into the respective equations along with regression coefficients (R^2). On the basis of the R^2 analysis, we concluded that in both mediums the Higuchi and power law models provided the best fits to the release kinetics data for FITC-BSA from ChS-HTCC NPs. It appears that FITC-BSA release is mainly controlled by the diffusion and Fickian transport process. A similar release mechanism to FITC-BSA in both mediums indicates that the pH has little influence on the ionic interaction between anionic protein and cationic HTCC.

3.6. Cell viability/cytotoxicity studies and uptake studies in vitro

Many medications are given via intravenous injection because of the rapid drug delivery and uptake effect. The endothelial cells, lining the lumen of blood vessels, are the first cells to contact a drug when it is injected into a vessel. To determine the cytotoxicity of ChS-HTCC NPs in endothelial cells, we used primary endothelial cells obtained from humans (HUVECs) instead of the immortal cell line. For the cell viability assessment, HUVECs were incubated with positively and negatively charged ChS-HTCC NPs for 24 h and assessed with an MTS assay. Our data showed that more than 80% of the cells were viable after incubation with charged ChS-HTCC NPs at various concentrations (Figure 6), indicating that charged ChS-HTCC NPs were not cytotoxic towards HUVECs. This suggests that charged ChS-HTCC could be a potential carrier for genes or drugs via intravenous administration.

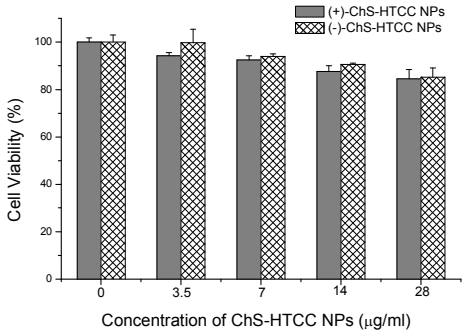

Figure 6. Effect of positively and negatively charged ChS-HTCC NPs on viability of human umbilical endothelial cells (HUVECs). HUBECs were treated with 0 (control), 3.5, 7, 14, or 28 μg/mL ChS-HTCC NPs for 24 h. Cell viability was assessed using the CellTiter 96® Aqueous One Solution Cell Proliferation Assay (MTS). More than 80% of the cells were viable in each samples. Three independent experiments were carried out. Data are presented as the mean ± SD. (+)- ChS-HTCC NPs represents a positive charge and (-) a negative charge.

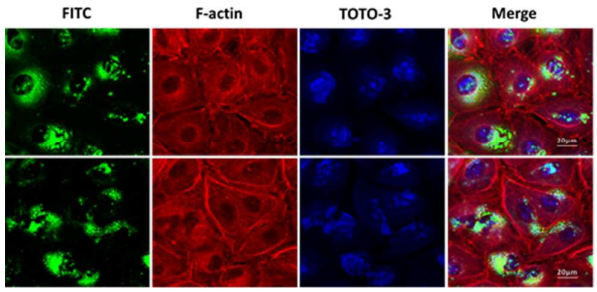

Figure 7. Cellular uptake and intracellular distribution of the positively (first line) and negatively charged (second line) ChS-HTCC NPs in A549 cells. A549 cells were cultured on 8-well chamber slides and treated with 7 μg/ml of positive or negative charged FITC-conjugated ChS-HTCC NPs (green) for 24 h at 37°C. The cytoskeleton was stained with Texas Red-X phalloidin, which represents the cytoplasm (red) and TOTO-3 was used as a nucleus stain (blue). Both charged ChS-HTCC NPs are enclosed in the cytoplasm. Three independent experiments were performed for both assays.

Furthermore, endocytosis is the critical step for applying the nanoparticle to gene or drug delivery in cancer treatment. Numerous studies have revealed that several chemo-physic properties could impact the cellular uptake behavior of nanoparticles including shape, size, and surface charge.[35,36] It has been reported that positively charged nanoparticles are taken up by the cells more easily because of the negatively charged cell membrane.[37-39] To investigate the uptake of charged ChS-HTCC NPs in cancer cells, confocal laser scanning imaging and flow cytometry were performed. After incubation with positively or negatively charged ChS-f-HTCC NPs for 24 hours, the A549 cell line was observed using confocal laser scanning. The images revealed that the majority of viable cells have bright fluorescent dots retained within the cytoplasm (Figure 7), indicating that the NPs were taken up by the cells. To quantify the efficiency of endocytosis of ChS-f-HTCC NPs, flow cytometry analysis was performed. Our data show that ChS-f-HTCC NPs were detected in more than 80% of the cells (Figure 8). This indicates that charged ChS-f-HTCC NPs can both penetrate and be retained by the cells efficiently.

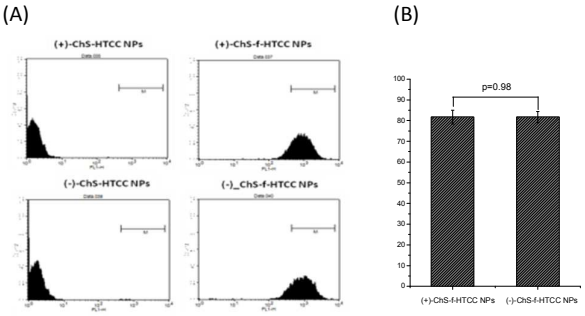

Figure 8. Quantification of positively and negatively charged ChS-HTCC NPs cellular uptake by A549 cells. Cells were incubated with 7 μg/ml of positively or negatively charged FITC-conjugated ChS-HTCC NPs for 24 h at 37°C on 6-well tissue culture plates. Then, cells were trypsinized and washed with PBS three times. Analysis of ChS-HTCC NPs by flow cytometry showed more than 80% fluorescent cells in both samples (K and L). (A) Representative flow cytometry of one set of triplicate experiments; (B) More than 80% of FITC-positive cells from flow cytometry analysis in both positively and negatively charged ChS-HTCC NPs. Three independent experiments were conducted for each kind of sample.

4. Conclusions

This study demonstrated that both positively and negatively surface charged NPs can be prepared using the PEC method of the ChS-HTCC system. It can easily be predicted whether positively charged NPs, negatively charged NPs, or aggregates are formed during this process by calculating the weight ratio of ChS/HTCC in the final concentration. A high encapsulation efficiency of anionic FITC-BSA was only achieved in the positively charged ChS-CS NPs and was easily re-dispersed in water and HEPES medium without the assistance of a surfactant. The release profile of FITC-BSA from positively charged ChS-HTCC NPs indicated that a continued and controlled release process occurred. Charged ChS-HTCC NPs

showed no cytotoxicity in HUVEC cells. Furthermore, ex vivo cellular uptake studies using A549 cells showed that charged ChS-f-HTCC NPs were phagocytosed into the cells efficiently. Thus, this new ChS-HTCC NP system has potential as a carrier system for both cationic and anionic proteins.

Acknowledgements

Thanks to Ms. Chia-Ying Chien of Precious Instrument Center (National Taiwan University) for the assistance in TEM experiments. Financial support for this work was provided by the Ministry of Science and Technology (MOST 104-2623-E-016-002-D & MOST 104-2623-E-016-003-D), the National Defense Medical Center (MAB-104-100 & IPM-103-B3) and the Tri-Service General Hospital (TSGH-C103-024) of the Republic of China.

Notes and references

1 S. A. Agnihotri, N. N. Mallikarjuna, T. M. Aminabhavi, J. Controlled Release, 2004, 100, 5-28.
2 T. A. Sonia and C. P. Sharma, Adv. Polym. Sci., 2011, 243, 23–54.
3 C. W. Nam, Y. H. Kim and S. W. Ko, J. Appl. Polym. Sci., 1999, 74, 2258–2265.
4 J. Huanga, H. Jianga, M. Qiua, X. Genga, R. Yanga, J. Li and C. Zhang, Int. J. Biol. Macromol., 2013, 52, 85–91.
5 Z. Penga, L. Wang, L. Du, S. Guo, X. Wang and T. Tang, Carbohydr. Polym., 2010, 81, 275–283.
6 X. Zhang, X. Geng, H. Jiang, J. Li and J. Huang, Carbohydr. Polym., 2012, 89, 486–491.
7 C. Bottegoni, R. A. A. Muzzarelli, F. Giovannini, A. Busilacchi and A. Gigante, Carbohydr. Polym., 2014, 109, 126–138.
8 M. Iouv, G. Dumais and P. Du Souich, Osteoarthritis Cartilage, 2008, 16, S14–18.
9 S. Cai, Y. Liu, X. Z. Shu and G. D. Prestwich, Biomaterials, 2005, 26, 6054–6067.
10 J. J. Lim, T. M. Hammoudi, A. M. Bratt-Leal, S. K. Hamilton, K. L. Kepple, N. C. Bloodworth, T. C. McDevitt and J. S. Temenoff, Acta Biomater., 2011, 7, 986–995.
11 J. S. Park, H. J. Yang, D. G. Woo, H. N. Yang, K. Na and K. H. Park, J. Biomed. Mater. Res. A, 2010, 92, 806–816.
12 S. Varghese, N. S. Hwang, A. C. Canver, P. Theprungsirikul, D. W. Lin and J. Elisseeff, Matrix. Biol., 2008, 27, 12–21.
13 B. C. Baudner, M. M. Giuliani, J. Coos Verhoef, R. Rappuoli, H. E. Junginger and G. D. Giudice, Vaccine, 2003, 21, 3837–3844.
14 D. Vllasaliu, R. Exposito-Harris, A. Heras, L. Casettari, M. Garnetta, L. Illumd and S. Stolnik, Int. J. Pharm., 2010, 400, 183–193.
15 P. Calvo, C. Remunan-Lopez, J. L. Vila-Jato and M. J. Alonso, J. Appl. Polym. Sci., 1997, 63, 125–132.
16 P. Calvo, C. Remunan-Lopez, J. L. Vila-Jato and M. J. Alonso, Pharm. Res., 1997, 14, 1431–1436.
17 S. K. Motwani, S. Chopra, S. Talegaonkar, K. Kohli, F. J. Ahmad and R. K. Khar, Eur. J. Pharm. Biopharm. 2008, 68, 513–525.
18 Z. Liu, Y. Jiao, F. Liu and Z. Zhang, J. Biomed. Mater. Res., 2007, 83A, 806–812.
19 F. A. Oyarzun-Ampuero, J. Brea, M. I. Loza, D. Torres and M. J. Alonso, Int. J. Pharm., 2009, 381, 122–129.
20 M. K. Yeh, K. M. Cheng, C. S. Hu, Y. C. Huang and J. J. Young, Acta Biomater., 2011, 7, 3804–3812.
21 Y. J. Park, Y. M. Lee, J. Y. Lee, Y. J. Seol, C. P. Chung and S. J. Lee, J. Controlled Release, 2000, 67, 385–394.
22 F. L. Mi, S. S. Shyu, C. K. Peng, Y. B. Wu, H. W. Sung, P. S. Wang and C. C. Huang, J. Biomed. Mater. Res., 2006, 76A, 1–15.
23 S. H. Lim and S. M. Hudson, Carbohydr. Res. 2004, 339, 313–319.
24 M. Huang, Z. Ma, E. Khor and L. Y. Lim, Pharm. Res., 2002, 9, 1488–1494.
25 R. K. Das, N. Kasoju and U. Bora, Nanomed.: Nanotechnol. Biol. Med., 2010, 6, 153-160.
26 S. C. Angadi, L. S. Manjeshwar, and T. M. Aminabhavi, Ind. Eng. Chem. Res., 2011, 50, 4504-4514.
27 T. Higuchi, J. Pharm. Sci., 1963, 53, 1145-1149.
28 K. G. Yeboah and M. J. D'souza, J. Microencapsulation, 2009, 26, 166-179.
29 J. Siepmann and N. A. Peppas, Adv. Drug Deliv. Rev., 2001, 48, 139-157.
30 R. W. Korsmeyer, R. Gurny, E. Doelker, P. Buri and N. A. Peppas, Int. J. Pharm., 1983, 15, 25-35.
31 P. L. Ritger and N. A. Peppas, J. Controlled Release, 1987, 5, 23-36.
32 P. L. Ritger and N. A. Peppas, J. Controlled Release, 1987, 5, 37-42.
33 J. J. Young, K. M. Cheng, T. L. Tsou, H. W. Liu and H. J. Wang, J. Biomater. Sci. Polymer. Edn., 2004, 15, 767-780.
34 R. Fernández-Urrusuno, P. Calvo, P. Remuñán-López, J. L. Vila-Jato and M. J. Alonso, Pharm. Res., 1999, 16, 1576-1581.
35 M. Motskin, D. M. Wright, K. Muller, N. Kyle, T. G. Gard, A. E. Porter and J. N. Skepper, Biomaterials, 2009, 30, 3307–3317.
36 L. Hu, Z. Mao, C. Gao, J. Mater. Chem. 2009, 19, 3108–3115.
37 S. E. A. Gratton, P. A. Ropp, P. D. Pohlhans, J. C. Luft, V. J. Madden, M. E. Napier and J. M. Desimone, Proc. Natl. Acad. Sci. U. S. A., 2008, 105, 11613–11618.
38 L. Chen, J. M. Mccrate, J. C. Li and H. Lee, Nanotechnol., 2011, 22, 105708.
39 C. A. Fromen, G. R. Robbins, T. W. Shen, M. P. Kai, J. P. Ting and J. M. DeSimone, Proc. Natl. Acad. Sci. U. S. A., 2015, 112, 488-493.

Positively and negatively surface charged nanoparticles were prepared by a facile PEC method composed of chondroitin sulfate and N-[(2-hydroxy-3-trimethylammonium)propyl]chitosan.